


CNT-based sensor arrays for local strain measurements in soft pneumatic actuators

Thassyo Pinto¹  · Le Cai¹ · Chuan Wang¹ · Xiaobo Tan¹

Received: 20 November 2016 / Accepted: 29 March 2017 / Published online: 21 April 2017
© Springer Singapore 2017

Abstract Soft robotics is a recent trend in engineering that seeks to create machines that are soft, compliant, and capable of withstanding damage, wear and high stress. Soft pneumatic actuators (SPAs) are a key element of soft robots, and their elastomeric substrate enables generation of sophisticated motion with simple controls. Although several methods for fabrication, material selection, and structure design have been investigated for the construction of SPAs, limited attention has been paid to the integration of distributed sensors for performing localized measurement. Carbon nanotubes (CNTs) are molecular-scale tubes of carbon atoms with remarkable mechanical and electronic properties, showing potential application in sensing devices. In this paper, we present the design, fabrication, and testing of a novel type of CNT-based sensor array combined with silver nanowires for measuring localized strain along the bottom layer of a SPA. Simulation and experimentation have been performed in order to analyze the soft actuator deformation during bending. The results demonstrate the promise of the proposed SPA with

integrated strain sensing, which lays groundwork for a myriad of applications in grasping, manipulation, and bio-inspired locomotion.

Keywords Soft robotics · Strain sensor array · CNT · Integrated sensing

1 Introduction

Traditionally, robots are composed of rigid bodies made from stiff materials such as metals and ceramics. These robots are widely applied in industry and can be preprogrammed to execute specific tasks with efficiency, but with constrained adaptability. The soft malleable state of elastomeric materials can enable a robot to readily adapt to different scenarios, facilitating tasks such as grasping (Brown et al. 2010) and improving mobility in unstructured and cluttered environments (McMahan et al. 2006). A soft robot is primarily made of soft and extensible materials such as silicone rubbers (Shepherd et al. 2011), synthetic fibers (Trivedi et al. 2008), or gels (Otake et al. 2002), enabling large deformation and absorption of energy generated from impacts. The highly deformable components allow the system to experience theoretically infinite degrees of freedom. In addition, the compliant structure mitigates the impact of environmental uncertainty and produces complex motion with simple control inputs. In contrast to their rigid counterparts, soft robots can often be fabricated with simple designs and inexpensive and lightweight materials.

The soft robotics literature is growing every day. These soft machines could contain single or multiple soft elements, such as bending actuators (Wakimoto et al. 2009), stretchable circuits (Rogers et al. 2010), and deformable

Electronic supplementary material The online version of this article (doi:10.1007/s41315-017-0018-6) contains supplementary material, which is available to authorized users.

✉ Thassyo Pinto
thassyo@msu.edu

Le Cai
lecai@msu.edu

Chuan Wang
cwang@msu.edu

Xiaobo Tan
xbtan@egr.msu.edu

¹ Department of Electrical and Computer Engineering,
Michigan State University, East Lansing, MI, USA

sensors (Park et al. 2010). Soft robotic mechanisms can potentially be applied in many different areas, such as manufacturing (Amend et al. 2012), medicine (Cianchetti et al. 2014), assistive technologies (Polygerinos et al. 2015), and bio-inspired robotics (Laschi et al. 2012). However, an existing challenge is the integration of sensing devices in the structure of a soft mechanism, for feedback control of the system. Several control schemes for soft robotic systems have been explored by researchers (Duriez 2013; Marchese et al. 2014; Vikas et al. 2015) however, feedback control of soft robots using compact, integrated sensors is generally limited. A tactile sensor sleeve based on fiber-optic light modulation (Sareh et al. 2014) can be incorporated in the body of a soft manipulator for pressure sensing; however, large instrumentation devices are required for measuring the light intensity variation. Commercially available sensors can be embedded in a soft pneumatic actuator skin (Suh et al. 2014), but their size and shape cannot be customized for various applications. Although previous works have investigated the use of eGaIn-filled microchannels (Park 2013; Bilodeau et al. 2015) on soft actuators for measuring deformation, the type of sensor configuration investigated does not allow gathering of localized data about the deformed structure. In a more recent study (Morrow et al. 2016), multiple soft strain sensors made of eGaIn were integrated along a SPA structure, but this injecting process can be challenging and lead to entrapped air inside the sensing layer. By using sensors built in an integrated circuit (IC) the sensing accuracy can be increased (Ozel et al. 2016), but its rigid parts can compromise the flexibility of the soft-bodied device.

In this paper, we present the design, fabrication, and testing of a novel strain sensor array for measuring the deformation at different locations of a SPA. The actuator is fabricated with a soft lithography process, while the CNT-based sensor array and their AgNWs electrode traces are fabricated through a screen-printing process over a polymeric substrate. The screen-printing process has the advantage of being simple and scalable. The sensor design can be customized, characterized and used for detecting the soft actuator deformation. As a demonstration, a sensor array with three strain gauges was fabricated, and bonded to the bottom layer of a SPA. Different actuation tests were performed in order to analyze the sensor array response. The obtained sensor measurements showed good correlation with the actual SPA deformation.

The remainder of this paper is organized as follows. In Sect. 2, we describe the fabrication processes for both the soft actuator and flexible sensor devices. In Sect. 3, the characterization of the sensor array is presented as long with the finite element analysis of the soft actuation mechanism. Section 4 provides discussion based on the

results obtained from this work, and concluding remarks are presented in Sect. 5.

2 Methodology

2.1 Fabrication of the soft actuator

The structure of a soft robot and its soft mechanisms can use several rubber-like materials. Similarly, there are different fabrication processes available for creating compliant robotic components such as soft lithography (Ilievski et al. 2011), 3D-printing (Peele et al. 2015), and photopatterning (Breger et al. 2015). In particular, we have studied the fabrication of soft bending actuators using a soft lithography process.

A soft lithography process can be divided into three main steps: material preparation, vacuum degassing, and curing. The specific shape of the actuator is achieved through the design of a mold. Our mold was designed on a CAD software (SolidWorks, Dassault Systemes) and had a square cross-section of 25×20 mm and length of 100 mm. As shown in Fig. 1a, the SPA design included topographical features, a similar concept as in (Mosadegh et al. 2014), and with 70° angle to allow higher bending. The mold was made of polylactic acid (PLA) thermoplastic and fabricated with a 3D printer (MakerBot Replicator, MakerBot Industries). In order to facilitate the removal of the soft actuator after the curing process, we designed a 2-part mold with molded-in assembly features (Fig. 1b). We first mixed a two-part liquid silicone rubber (Dragon Skin 30, Smooth-On) and filled the mold with the uncured material. The silicone was then degassed in a vacuum chamber and allowed to cure for 16 h at the room temperature. Once the curing process was completed, the soft actuator was removed from the mold and its open ends were sealed with uncured silicone. In order to supply compressed air to the soft actuator chambers (see Fig. 1c), a silicone-based tubing with similar durometer (3.175 mm diameter) was inserted through the bottom layer of the actuator structure.

2.2 Fabrication of the flexible sensor

In this work, we investigate new methods for achieving flexible sensors that can detect strains along a soft bending actuator. In Fig. 2, we demonstrate how a CNT-based sensor array can be fabricated through simple steps. This design allows the creation of customizable flexible sensors without geometric constraints.

An array of CNT-based strain gauges was fabricated using a screen-printing process. A polyimide film (Kapton, DuPont) was used for designing the pattern of the sensor

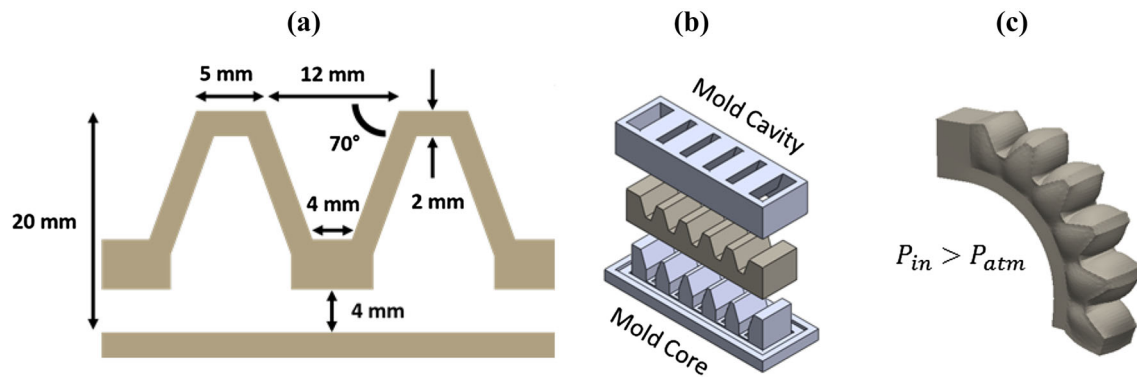


Fig. 1 Design approach for the soft actuator and mold parts. **a** Cross-section of the SPA with the corresponding dimensions; **b** core and cavity sides of the 3D printed mold; **c** inflation state of the SPA

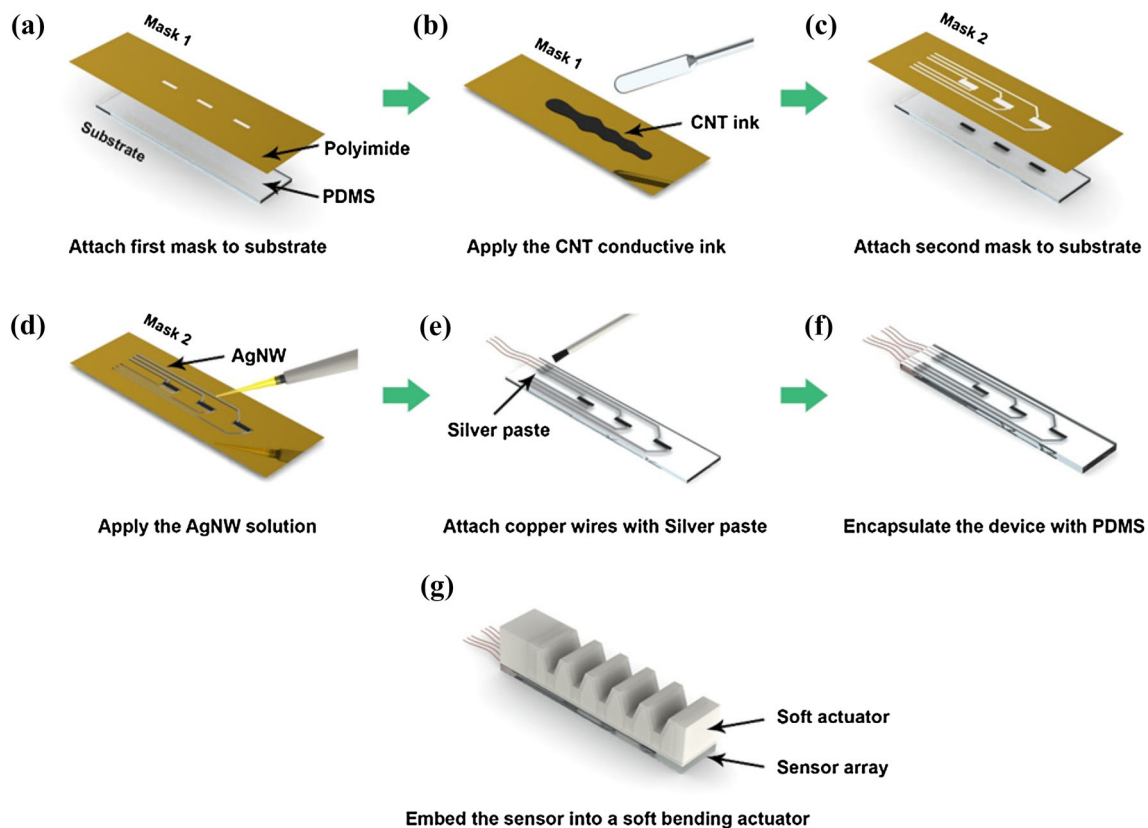


Fig. 2 Fabrication steps of the flexible CNT-based sensor array: **a** the sensor mask is attached to the polymeric substrate; **b** the CNT conductive ink is applied over the mask surface to create the distributed strain sensors; **c** the trace mask is attached to the substrate;

d AgNW solution is applied through the mask gaps using a pipette; **e** thin copper wires are attached to the endpoint of each trace with a silver paste; **f** encapsulation of the device with PDMS; **g** and bonding of SPA and sensor array with uncured silicone

array and circuit traces. In the first mask, we cut three equally spaced rectangles (10×2 mm) corresponding to the areas for the distributed sensor array along the device structure. A second mask was created to assist in the application of the trace material, with each sensor connected to two traces on its ends. The material used for the sensor substrate was polydimethylsiloxane (PDMS) (Sylgard 184, Dow Corning) with a 10:1 base and agent mix

ratio. The substrate (≈ 2 mm thickness) was fabricated using two heat-resistant borosilicate glass sheets (150×150 mm) clamped together and heated over a hot plate for 10 min at 150°C . A polyester film was adhered to the inner surface of each glass sheet to help in the removal of the PDMS substrate without causing any tear or wrinkles. The size and shape of the spacer material directly affect the substrate uniformity. In this procedure, we have

used microscope slides with identical width and length to separate the glass sheets at opposite edges. After fabrication, the substrate was cut in a rectangular shape (120 × 25 mm) and treated with electric discharge to convert it to a less hydrophobic surface (wetting). The substrate and the first mask were attached together to allow the application of the sensor material (Fig. 2a). A single-walled CNT (SWCNT) conductive ink, 1 mg/mL CNTs (VC101, Chasm Technologies), was applied over the polyimide film (Fig. 2b), allowing the deposition of the SWCNTs on the PDMS substrate only through the small cuts. Small variations on ink dispersion can cause deviation in sensing characteristics. A spatula was used to level the CNT paste even with the polyimide film to obtain an ideal dispersion at each sensor location. The substrate was once again heated (60 °C) in order to ensure adhesion between both materials. Once dried, the second mask was attached to the substrate (Fig. 2c). AgNWs in water (AgNW50H2O, ACS Material), with 50 nm of diameter and 200 µm of length, was applied through the open cuts using a pipette (see Fig. 2d). The traces were dried at 60 °C for 1 h. As shown in Fig. 2e, thin copper wires were attached to the endpoints of each trace by fixing them with a silver paste, 60% Ag (PELCO Colloidal Silver, Ted Pella). A second layer of uncured PDMS was applied to the top face of the sensor array to encapsulate the device (Fig. 2f).

As an example, the sensor array was fabricated with three strain gauges which are referred to as S_1 , S_2 and S_3 in this work, with S_1 being closest to the air inlet, and S_3 being close to the distal end of the actuator. The flexible sensor array was characterized (Sect. 3) and bonded to the bottom surface of the soft actuator using uncured PDMS (Fig. 2g). The fabricated devices are shown in Fig. 3.

2.3 Strain measurement

The CNT conductive ink has a mesh-like nanostructure which can change its electronic characteristics when subjected to extension or compression. When there is a voltage between both ends of an individual CNT-based sensor, the latter behaves as a variable resistor that changes its resistance

value during mechanical deformation. A voltage divider circuit can be used to measure the voltage across the flexible strain gauge sensor and thus its resistance value. By using Ohm's Law, we have:

$$V_s = I_s \times R_s, \quad (1)$$

$$I_s = \frac{V_i}{R_{ref} + R_s}, \quad (2)$$

where V_i , V_s are the input voltage and the voltage across the sensor, respectively, I_s is the current going through the sensor, and R_s and R_{ref} are the sensor resistance and the reference resistance, respectively. By combining (1) and (2), we can get,

$$R_s = \frac{R_{ref}}{\left(\frac{V_i}{V_s} - 1\right)}. \quad (3)$$

The resistance R_{ref} is selected based on the minimum and maximum resistance values obtained from each individual sensor (denoted as $R_{s,min}$ and $R_{s,max}$, respectively). This relation can be expressed as:

$$R_{ref} \approx \sqrt{R_{s,min} \times R_{s,max}}. \quad (4)$$

In order to associate the change in resistance with the amount of strain applied at a sensor position, multiple measurements of the resistance are recorded as the substrate is subjected to different values of strain. The axial strain formula is given by:

$$\varepsilon = \frac{\Delta L_s}{L_{so}} = \frac{L_s - L_{so}}{L_{so}}, \quad (5)$$

where L_{so} and L_s are the nominal (untensioned) length and the current length of the sensor array, respectively.

3 Results

3.1 Sensor characterization

The fabricated CNT-based sensor array was placed on a programmable stretching device with both ends clamped (80 mm active length). A loading cycle of ≈ 10 s (stretch

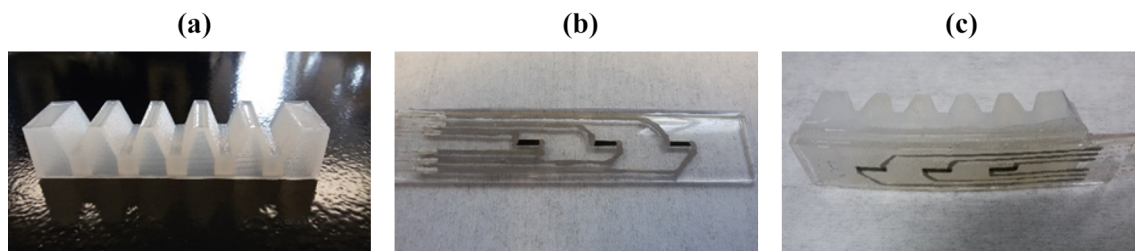


Fig. 3 The fabricated devices. **a** SPA, **b** CNT-based sensor, and **c** both devices bonded together

and release) was performed for 60 min for the initial conditioning step of the device (Fig. 4). The sensor array was subjected to a stretch of 5% ($L_s = 84$ mm). This is an important process for stabilizing the microscale structural change of the nanomaterials. The conditioning phase was performed until the device achieved reversible and stable electrical signals for a desired range of strain. Although the sensor array had reached its stability margin after 60 min, the stretching cycle was run up to ≈ 180 min to ensure measurement repeatability. A data acquisition equipment was used in combination with an integrated dataflow software (LabVIEW, National Instruments) for collecting the change in resistance of each strain sensor.

After the conditioning step, each individual sensor was measured in a sequence. In Fig. 5, we show a short sample of the collected data from sensors S_1 to S_3 after 96 min of stretching. Each strain gauge experienced different ranges of resistance change since the concentration of the CNT material and the thickness along the substrate can directly affect their measurement range. The sensors fabricated in this work were tested only for stretches below 10%. A larger strain value could increase the number of cracks in the sensors, causing malfunction and unreliable measurements. Other design options that alleviate mechanical stress such as a horseshoe-shape would allow sensor functionality for larger stretches.

Based on the data collected from the stretching process, we obtained the resistance-strain relation (gauge factor) for each individual CNT-based sensor (Fig. 6). As is observed, all three sensors achieve a saturation level at a certain strain value. Since the CNT bundles change their arrangement when the substrate is under strain, the conductive path within the nanomaterial is modified. The change in each sensor's shape during stretching can also

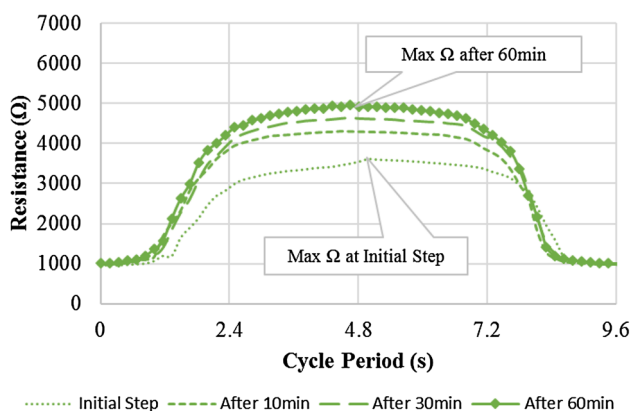


Fig. 4 Continuous measurement of the resistance change in S_1 during conditioning phase. The depicted lines show the difference in the maximum range of the sensor at initial step and after three time frames: 10, 30, and 60 min of loading cycle

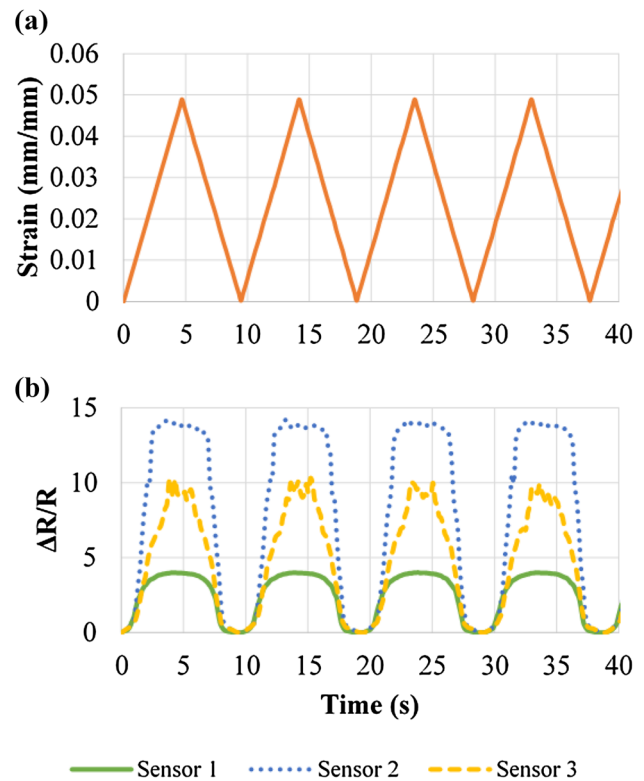


Fig. 5 Sensor array measurements after initial conditioning: **a** the amount of strain applied in the continuous stretch and release test, **b** and the relative change in resistance ($\Delta R/R$) for sensors S_1 , S_2 , and S_3

contribute to a saturated strain behavior. For small strain values, the gauge factor of each strain gauge is defined as:

$$GF = \frac{\Delta R/R}{\varepsilon} = \frac{\Delta R_s/R_{so}}{\Delta L_s/L_{so}} = \frac{\Delta R_s L_{so}}{R_{so}(L_s - L_{so})}. \quad (6)$$

3.2 Soft actuator simulation

Simulation of soft actuators and flexible sensors is an important process in the study of soft robotic systems, in order to analyze their mechanical behavior, frequency response and design performance. A Finite Element Method (FEM) model captures the nonlinearity of the system, but its complexity can lead to high computational cost. We have simulated several soft bending actuator prototypes, using a finite element analysis software (Abaqus/CAE, Dassault Systemes). The geometries of the soft actuator and the sensor substrate were designed as solid bodies and meshed using solid tetrahedral quadratic hybrid elements (C3D10H element type), with 48,253 nodes and 30,144 elements. The Dragon Skin 30 and PDMS materials were modeled as an incompressible Yeoh material ($\mu = 2.38$ kPa) (Elsayed et al. 2014) and incompressible Neo-Hookean material ($\mu = 1.84$ MPa) (Martinez et al. 2013), respectively. As shown in Fig. 7a, the simulated soft

Fig. 6 Gauge factor of each strain gauge. **a** Strain and $\Delta R/R$ relationship based on different sets of data (with mean lines) obtained through the cyclic stretching of the sensor array substrate, **b** and the standard deviation of $\Delta R/R$ from the measured samples

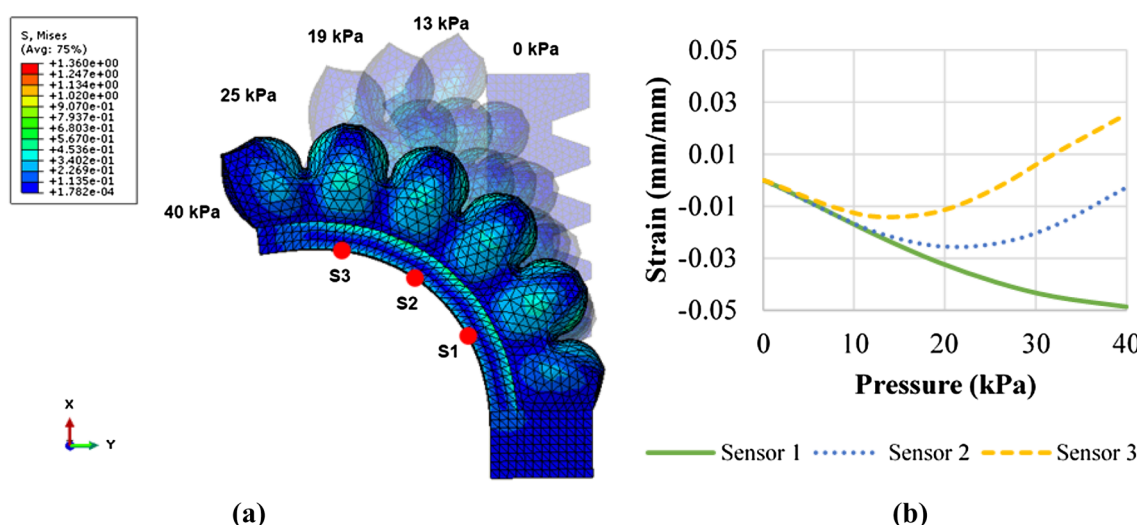
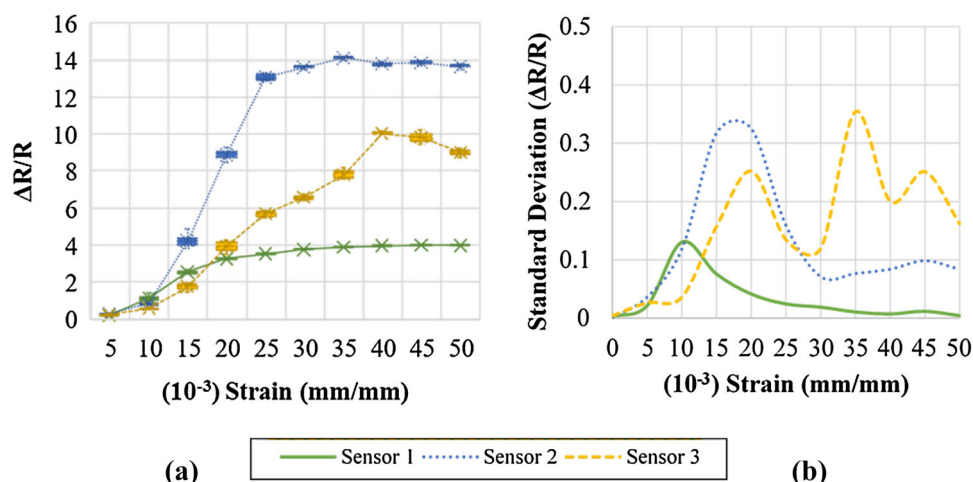


Fig. 7 Finite element simulation of the SPA. **a** Contour plot of the SPA FEM model (DragonSkin/PDMS), and its sequential deformation as pressure increases. **b** Graph of the strain values at each node corresponding to a sensor location

bending actuator achieved a quarter bending when a pressure of 40 kPa (≈ 5.8 psi) was applied to its inner chamber. The nodes 4455, 4365 and 4275 at the bottom surface were selected as the position for the strain gauges S_1 , S_2 and S_3 , respectively. The uniaxial strains at the nodes that corresponded to the locations of the strain sensors were measured in the converged solution (Fig. 7b).

3.3 Actuator-sensor testing

The performance of the integrated soft actuator-sensor was evaluated in experiments. In this procedure, the sensor S_2 was not included since the process of embedding the sensor array substrate with the SPA caused a malfunction of this sensor. A pressure gauge sensor (ASDX Series, Honeywell) was used for detecting the inner pressure of the soft pneumatic actuator during the bending motion. The soft actuator inlet was connected to a 12VDC miniature air

compressor ($P_{max} = 28$ psi) through a polyurethane tubing. During this test, we measured the resistance change of S_1 and S_3 . When the sensor array was combined with the soft actuator, the minimum and maximum resistance values were changed due to the contribution of residual strain from the soft structure. By measuring R_{s1} and R_{s3} with a multimeter during the actuator inflation, we registered the new values as: $R_{s1,min} \approx 1.3$ k Ω and $R_{s1,max} \approx 2.7$ k Ω ; $R_{s3,min} \approx 1.8$ k Ω and $R_{s3,max} \approx 3.6$ k Ω . From Eq. (4), we obtained the value for the reference resistors as $R_{ref,s1} \approx 1.8$ k Ω , $R_{ref,s3} \approx 2.4$ k Ω , and a series circuit was built using trim potentiometers.

The sensor outputs (pressure and strain gauges) were sent to a microcontroller (MEGA 2560, Arduino), which was connected to a computer using USB interface for communication with the data acquisition software. All measurements were obtained with a sampling time of ≈ 25 ms, and a solenoid valve connected to an air pump

was controlled using pulse-modulation width (PWM) at 50 Hz. As shown in Fig. 8a, the fabricated soft actuator achieved 90° bending angle with an internal pressure of 60 kPa (≈ 8.7 psi), which is close to the FEM simulation results. The curvature of the soft actuator inner radius was captured with a digital camera, recording individual frames that correspond to a constant pressure value. The percentage of the PWM duty cycle was computed by a PID function within LabVIEW, with the process variable being the median of the pressure sensor output after thirty measurements. Various setpoints were tested with the control system, and the respective resistance values in each strain gauge were captured, as shown in Fig. 8b.

The SPA can be applied in several tasks such as reaching, grasping and touching. In order to have an accurate estimation about the actuator position or curvature, the sensor array must be able to capture the deformation during motion. In Fig. 9a, b, we show the measurements of the difference in the sensor output response (hysteresis) during inflation (loading) and deflation (unloading), with a range of pressure setpoints varying every 0.8 ms. The total operating time is 16 s, with the setpoint increasing from 0 to 60 kPa, and vice versa (Fig. 9c).

With the gauge factor obtained during the sensor array characterization process, we estimated the amount of strain in the SPA at different curvatures. The actual curvature of the SPA was measured from the captured image frames during bending. An image processing software (Vision Assistant, National Instruments) was used to measure the SPA inner radius of curvature for each pressure setpoint. The arc length of a specific bending shape was measured and inserted in Eq. (5) (with $L_{so} = 100$ mm) to find its correspondent axial strain value (ϵ). In Fig. 10, we compare

both sensor and actual measurements when the curvature increases. These results agree with the compression observed in the bottom layer of the SPA during positive pressure.

4 Discussion

4.1 Soft actuator curvature

Many different silicone rubber materials can be used for fabricating soft actuators. An elastomeric material is characterized by its durometer level (Shore Hardness). Low durometer silicones can resist extensive elongations, allowing the soft actuator to generate full bending curvature at low pressure values. By implementing the soft bending actuator and the integrated sensors with the aforementioned materials, the soft bending actuator was able to generate a 90° bending angle with pressure values less than 60 kPa.

4.2 Sensor substrate thickness

The constraint layer of a soft bending actuator, which in this work was considered as the substrate of the sensor array, can directly affect the actuator performance (bending curvature) when its thickness value is changed. A thinner layer will enable the actuator to require less pressure in order to achieve full bending. On the other hand, decreasing the thickness of the substrate brings a challenge to the fabrication of the sensor device since the uncured silicone dispersion creates a nonuniform surface. This causes a drastic variation among the characterizations of each strain gauge in the sensor array. Moreover, it

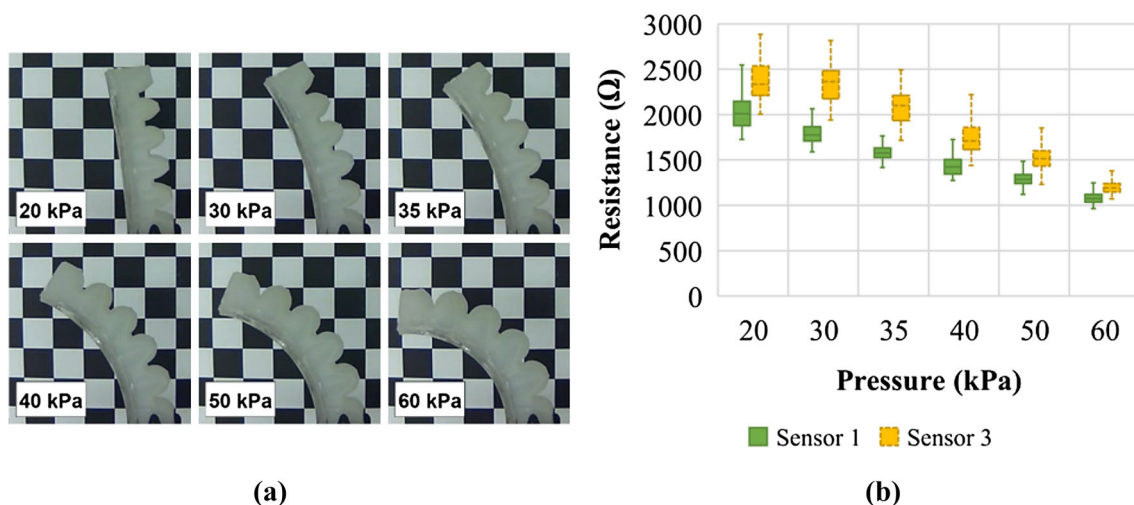


Fig. 8 The sequence of images of the SPA with embedded CNT-based sensors, showing the curvature and sensor values at different applied pressures. **a** Captured images during activation of the SPA, and **b** the strain gauge array measurement at various constant pressure setpoints

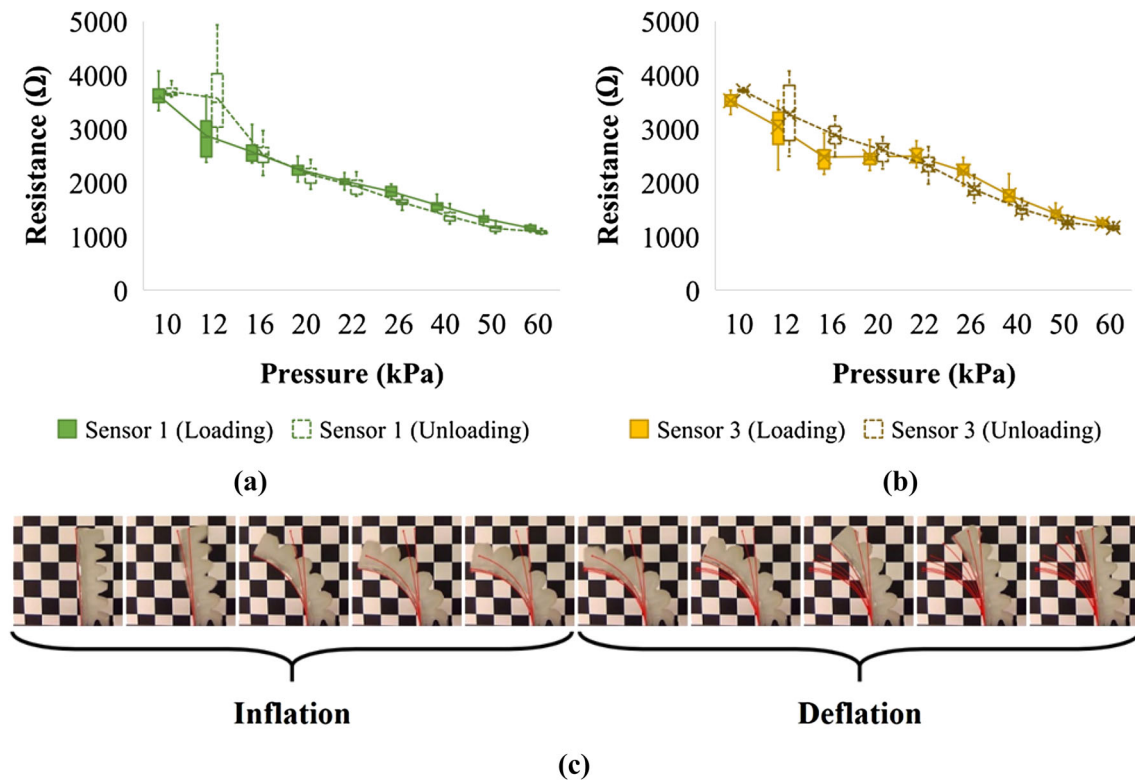


Fig. 9 Pressure and resistance relationship for the fabricated SPA with embedded sensor array. The variation in resistance (with mean lines) for both inflation (loading) and deflation (unloading) steps are

shown for sensors S_1 (a) and S_3 (b), when the pressure setpoint was varying from 0 to 60 kPa. **c** A sequence of *frames* showing the actuation steps and the curvature of the SPA

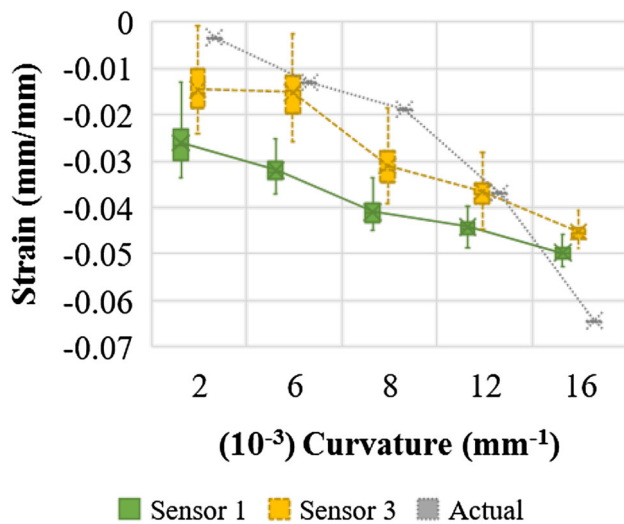


Fig. 10 The relationship between strain and curvature of the SPA based on the range of resistance values captured by the sensor array. The actual value represents the measured curvature from the SPA inner radius

generates difficulty in predicting the gauge factor for each sensor, which removes the possibility of a single circuit design (same R_{ref}) for all sensors in a voltage divider configuration.

4.3 Sensor array

By integrating multiple strain gauges along the soft actuator structure, the sensor array can provide angular measurement, contact detection or proprioceptive sensing for a soft robotic system. The distributed measurements allow estimation of the actuator deformation and the locations and forces of interactions between the actuator and foreign objects. Since the sensors are fabricated through screen-printing process, customization can be applied according to the soft actuator geometry and strain directions of interest. In addition, the number of strain sensors and their position can be optimally chosen based on the regions which experience large deformations. The sensor array design presents some constraints regarding the number of sensors that can be fabricated in a single substrate. Since the trace width can affect the sensor reading, reducing its dimension to increase the amount of strain gauges can impact the reliability of the sensor measurement. Increasing the thickness of each trace may allow the design of thinner features, but this process was not investigated in this current work. The manual fabrication method applied in this work brings challenges for achieving a uniform substrate thickness and CNT ink dispersion. Automated mass production ultraviolet (UV) curing and screen-printing

processes could reduce the uncertainties and issues identified in the investigated method.

5 Conclusions

We investigated the design and fabrication of CNT-based strain sensors that can be embedded in the structure of a soft robotic component. An array of strain gauges can be used as a distributed sensor network along the compliant mechanism. The sensor size and shape can be customized for many different applications. In this work, we tested the CNT-based strain sensor for detecting deformation at different locations at the bottom surface of a SPA. The results provide initial steps in the implementation of a sensor array for monitoring local deformation on a soft robotic mechanism.

There are several directions for extending the presented work. We are working towards new types of soft robotic actuators that can exploit sensing capabilities integrated in their mechanical structure. More investigation needs to be performed in order to achieve better uniformity on the sensor substrate and ink dispersion, which will facilitate the characterization process of multiple embedded sensors. While the present work focused on single-degree-of-freedom strain measurement, future work involves the study of sensor arrays for multi-axis measurements. Furthermore, the integrated strain gauges will be used in feedback control of the SPA to achieve accurate displacement and force control.

Acknowledgements This work was supported by Coordenação de Aperfeiçoamento de Pessoal de Nível Superior (CAPES) under the Science Without Borders program (BEX-13404-13-0) and National Science Foundation (DBI-0939454 and ECCS-1549888).

References

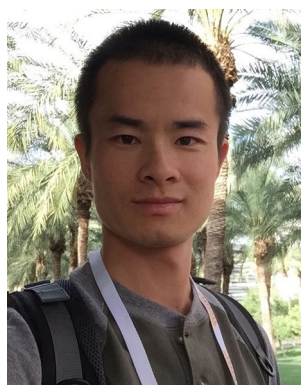
- Amend, J.R., Brown, E., Rodenberg, N., Jaeger, H.M., Lipson, H.: A positive pressure universal gripper based on the jamming of granular material. *IEEE Trans. Robot.* **28**(2), 341–350 (2012)
- Bilodeau, R.A., White, E.L., Kramer, R.K.: Monolithic fabrication of sensors and actuators in a soft robotic gripper. In: *Intelligent Robots and Systems (IROS)*, 2015 IEEE/RSJ International Conference on, Hamburg, Germany (2015)
- Breger, J.C., Yoon, C., Xiao, R., Kwag, H.R., Wang, M.O., Fisher, J.P., Nguyen, T.D., Gracias, D.H.: Self-folding thermo-magnetically responsive soft microgrippers. *ACS Appl. Mater. Interfaces.* **7**(5), 3398–3405 (2015)
- Brown, E., Rodenberg, N., Amend, J., Mozeika, A., Steltz, E., Zakin, M.R., Lipson, H., Jaeger, H.M.: Universal robotic gripper based on the jamming of granular material. *Proc. Natl. Acad. Sci.* **107**(44), 18809–18814 (2010)
- Cianchetti, M., Ranzani, T., Gerboni, G., Nanayakkara, T., Althoefer, K., Dasgupta, P., Menciassi, A.: Soft robotics technologies to address shortcomings in today's minimally invasive surgery: the STIFF-FLOP approach. *Soft Robot.* **1**(2), 122–131 (2014)
- Duriez, C.: Control of elastic soft robots based on real-time finite element method. In: *Robotics and Automation (ICRA)*, 2013 IEEE International Conference on, Karlsruhe, Germany (2013)
- Elsayed, Y., Vincensi, A., Lekakou, C., Geng, T., Saaj, C.M., Ranzani, T., Cianchetti, M., Menciassi, A.: Finite element analysis and design optimization of a pneumatically actuating silicone module for robotic surgery applications. *Soft Robot.* **1**(4), 255–262 (2014)
- Ilievski, F., Mazzeo, A.D., Shepherd, R., Chen, X., Whitesides, G.M.: Soft robotics for chemists. *Angew. Chem.* **123**(8), 1930–1935 (2011)
- Laschi, C., Cianchetti, M., Mazzolai, B., Margheri, L., Follador, M., Dario, P.: Soft robot arm inspired by the octopus. *Adv. Robot.* **26**(7), 709–727 (2012)
- Marchese, A.D., Komorowski, K., Onal, C.D., Rus, D.: Design and control of a soft and continuously deformable 2d robotic manipulation system. In: *Robotics and Automation (ICRA)*, 2014 IEEE International Conference on, Hong Kong, China (2014)
- Martinez, R.V., Branch, J.L., Fish, C.R., Jin, L., Shepherd, R.F., Nunes, R., Suo, Z., Whitesides, G.M.: Robotic tentacles with three-dimensional mobility based on flexible elastomers. *Adv. Mater.* **25**(2), 205–212 (2013)
- McMahan, W., Chitrakaran, V., Csencsits, M., Dawson, D., Walker, I.D., Jones, B.A., Pritts, M., Dienno, D., Grissom, M., Rahn, C.D.: Field trials and testing of the OctArm continuum manipulator. In: *Robotics and Automation*, 2006. ICRA 2006. Proceedings 2006 IEEE International Conference on, Orlando, Florida (2006)
- Morrow, J., Shin, H.-S., Phillips-Grafflin, C., Jang, S.-H., Torrey, J., Larkins, R., Dang, S., Park, Y.-L., Berenson, D.: Improving soft pneumatic actuator fingers through integration of soft sensors, position and force control, and rigid fingernails. In: *Robotics and Automation (ICRA)*, 2016 IEEE International Conference on, Stockholm, Sweden (2016)
- Mosadegh, B., Polygerinos, P., Keplinger, C., Wennstedt, S., Shepherd, R.F., Gupta, U., Shim, J., Bertoldi, K., Walsh, C.J., Whitesides, G.M.: Pneumatic networks for soft robotics that actuate rapidly. *Adv. Func. Mater.* **24**(15), 2163–2170 (2014)
- Otake, M., Kagami, Y., Inaba, M., Inoue, H.: Motion design of a starfish-shaped gel robot made of electro-active polymer gel. *Robot. Auton. Syst.* **40**(2), 185–191 (2002)
- Ozel, S., Skorina, E.H., Luo, M., Tao, W., Chen, F., Pan, Y., Onal, C.D.: A composite soft bending actuation module with integrated curvature sensing. In: *Robotics and Automation (ICRA)*, 2016 IEEE International Conference on, Stockholm, Sweden (2016)
- Park, Y.L., Majidi, C., Kramer, R., Bérard, P., Wood, R.J.: Hyperelastic pressure sensing with a liquid-embedded elastomer. *J. Micromech. Microeng.* **20**(12), 125029 (2010)
- Park, Y.L., Wood, R.J.: Smart pneumatic artificial muscle actuator with embedded microfluidic sensing. In: *SENSORS*, 2013 IEEE, Baltimore, Maryland (2013)
- Peele, B.N., Wallin, T.J., Zhao, H., Shepherd, R.F.: 3D printing antagonistic systems of artificial muscle using projection stereolithography. *Bioinspir. Biomim.* **10**(5), 055003 (2015)
- Polygerinos, P., Galloway, K.C., Savage, E., Herman, M., O'Donnell, K., Walsh, C.J.: Soft robotic glove for hand rehabilitation and task specific training. In: *Robotics and Automation (ICRA)*, 2015 IEEE International Conference on, Seattle, Washington (2015)
- Rogers, J.A., Someya, T., Huang, Y.: Materials and mechanics for stretchable electronics. *Science* **327**(5973), 1603–1607 (2010)
- Sareh, S., Jiang, A., Faragasso, A., Noh, Y., Nanayakkara, T., Dasgupta, P., Seneviratne, L.D., Wurdemann H.A., Althoefer, K.: Bio-inspired tactile sensor sleeve for surgical soft

- manipulators. In: Robotics and Automation (ICRA), 2014 IEEE International Conference on, Hong Kong, China (2014)
- Shepherd, R.F., Ilievski, F., Choi, W., Morin, S.A., Stokes, A.A., Mazzeo, A.D., Chen, X., Wang, M., Whitesides, G.M.: Multigait soft robot. *Proc. Natl. Acad. Sci.* **108**(51), 20400–20403 (2011)
- Suh, C., Margarit, J.C., Song, Y.S., Paik, J.: Soft pneumatic actuator skin with embedded sensors. In *Intelligent Robots and Systems (IROS 2014)*, 2014 IEEE/RSJ International Conference on, Chicago, Illinois (2014)
- Trivedi, D., Dienno, D., Rahn, C.D.: Optimal, model-based design of soft robotic manipulators. *J. Mech. Des.* **130**(9), 091402 (2008)
- Vikas, V., Grover, P., Trimmer, B.: Model-free control framework for multi-limb soft robots. In: *Intelligent Robots and Systems (IROS)*, 2015 IEEE/RSJ International Conference on, Hamburg, Germany (2015)
- Wakimoto, S., Ogura, K., Suzumori, K., Nishioka, Y.: Miniature soft hand with curling rubber pneumatic actuators. In: *Robotics and Automation, 2009. ICRA '09. IEEE International Conference on*, Kobe, Japan (2009)



Mr. Thassyo Pinto received his B.S. in Mechatronics Engineering from Universidade Salvador (UNIFACS), Brazil, in 2014. Throughout his academic life, he had the opportunity to work as a volunteer in various professional societies, promoting technology awareness for the community by organizing seminars, workshops and competitions. He has experience in automotive industry, working as a Vehicle Package engineer and as a Vehicle Evaluation and

Verification (VEV) Sign-off engineer at Ford Motor Company. He is now a Ph.D. student in Electrical Engineering at Michigan State University, and a member of the Smart Microsystems Lab and Adami Lab. His research interests are in soft robotics, evolutionary robotics and biorobotics. He is also an active member of the IEEE Robotics and Automation Society (RAS), acting as the Regional Student Representative (RSR) for Regions 1 to 7.



Dr. Le Cai received his Ph.D. in Condensed Matter Physics from the group of Prof. Sishen Xie (Academician, Chinese Academy of Sciences) in July 2014. He joined Michigan State University as a postdoctoral research scholar in August 2014. Dr. Cai's research interests include nanomaterials, nanoelectronics, flexible/stretchable electronics and printed electronics. He has extensive experiences in the controlled growth, physical

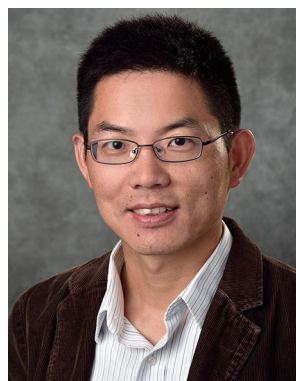
characterization and device applications of carbon nanomaterials. His

work at MSU has been focused on flexible and stretchable electronics by printing process. Dr. Cai has published 27 journal papers and one book chapter. He is an editorial member for MAYFEB Journal of Materials Science.



Dr. Chuan Wang joined Michigan State University as an assistant professor of Electrical and Computer Engineering in 2013. He received his Ph.D. in Electrical Engineering from University of Southern California in 2011 and worked as a postdoctoral scholar in the department of Electrical Engineering and Computer Sciences at UC Berkeley from 2011 to 2013. Dr. Wang's current research interests include: (1) low-cost fully-printed flexible

and stretchable electronics for displaying, sensing, and energy harvesting applications; and (2) high-performance nanoelectronics and optoelectronics using 2-dimensional semiconductors. He has published 43 journal papers with over 2600 citations and an h-index of 26. He also has 47 conference presentations, 19 invited presentations, 3 book chapters and 3 US patents. Dr. Wang serves as the associate editor for *Nanoscale Research Letters* and is an editorial board member for *Scientific Reports*.



Dr. Xiaobo Tan received the B.Eng. and M.Eng. degrees in automatic control from Tsinghua University, Beijing, China, in 1995 and 1998, respectively, and the Ph.D. degree in electrical and computer engineering from the University of Maryland, College Park, in 2002. From September 2002 to July 2004, he was a Research Associate with the Institute for Systems Research at the University of Maryland. He joined the faculty of the Department of

Electrical and Computer Engineering at Michigan State University (MSU) in 2004, where he is currently an MSU Foundation Professor. His research interests include modeling and control of systems with hysteresis, electroactive polymer sensors and actuators, soft robotics, and bio-inspired underwater robots and their application to environmental sensing. Dr. Tan has served as an Associate Editor/Technical Editor for *Automatica*, *IEEE/ASME Transactions on Mechatronics*, and *International Journal of Advanced Robotic Systems*. He served as the Program Chair of the 2011 International Conference on Advanced Robotics, and the Finance Chair of the 2015 American Control Conference. He has coauthored one book (*Biomimetic Robotic Artificial Muscles*) and over 80 journal papers, and holds one US patent. He was a recipient of NSF CAREER Award (2006), MSU Teacher-Scholar Award (2010), and several best paper awards.